Radiative lifetime and transition probabilities in CdI and CdII

Xu, Huailiang; Persson, Anders; Svanberg, Sune; Blagoev, K; Malcheva, G; Pentchev, V; Biemont, E; Campos, J; Ortiz, M; Mayo, R

Published in:
Physical Review A (Atomic, Molecular and Optical Physics)

DOI:
10.1103/PhysRevA.70.042508

2004

Radiative lifetime and transition probabilities in Cd I and Cd II

H. L. Xu, A. Persson, and S. Svanberg
Department of Physics, Lund Institute of Technology, P.O. Box 118, S-221 00 Lund, Sweden

K. Blagoev,* G. Malcheva, and V. Pentchev
Institute of Solid State Physics, 72 Tzarigradsko Chaussee, BG-1784 Sofia, Bulgaria

E. Biémont
Astrophysique et Spectroscopie, Université de Mons-Hainaut, 15 Rue de la Halle, B-7000 Mons, Belgium and IPNAS (Bât. B 15), Université de Liège, Sart Tilman, B-4000 Liège 1, Belgium

J. Campos, M. Ortiz, and R. Mayo
Department of Atomic, Molecular and Nuclear Physics, Universidad Complutense de Madrid, E-28040 Madrid, Spain
(Received 29 March 2004; revised manuscript received 16 June 2004; published 25 October 2004)

Radiative lifetimes of 11 levels belonging to the $5s5p\ ^1P^o_1$, $5snd\ ^3D_{1,2}$ ($n=6-9$) and $5sns\ ^3S_1$ ($n=7,8$) series of Cd I, and of 5 levels of Cd II (i.e., $4d^{10}5p\ ^2P^o_{1/2,3/2}$, $4d^{10}6s\ ^2S_{1/2}$, and $4d^{10}5d\ ^2D_{3/2,5/2}$) have been measured using the time-resolved laser-induced fluorescence technique. Free neutral and singly ionized cadmium atoms have been generated by laser ablation. Single- or two-step excitation processes were considered to populate the levels under study. Branching fractions of Cd II transitions have been measured by laser-induced breakdown spectroscopy. Transition probabilities and oscillator strengths for Cd I and Cd II spectral lines originating from the above states as well as from the $4d^95s^2\ ^2D_{3/2,5/2}$ states of Cd II have been deduced by combining the experimental lifetimes and theoretical branching fractions obtained in multiconfigurational relativistic Hartree-Fock calculations taking core-polarization effects into account.

DOI: 10.1103/PhysRevA.70.042508 PACS number(s): 32.70.Cs, 42.62.Fi

I. INTRODUCTION

Accurate atomic data such as radiative lifetimes and transition probabilities are of great interest in many fields of physics. From a theoretical point of view, they are sensitive to the electronic coupling schemes and to configuration interaction, and are thus important for testing the theoretical models [1]. In astrophysics, evaluation and extraction of information from observed stellar spectra heavily rely on the availability of atomic data [2,3]. In laser physics, lifetimes and transition probabilities are decisive for predictions of potential laser action in specific media [4]. The radiative properties of atoms and ions are also of great importance in plasma physics and in laser chemistry. In addition, atomic data of some elements, for example, of cadmium and zinc, are needed for development of high-quality and efficient light sources including metal-halide arc lamps and metal vapor lasers.

Among the methods available for lifetime measurements, very reliable ones are those based on selective excitation of the levels of interest, using, for example, a tunable laser. In contrast with collisional excitation methods, these techniques are free of cascading effects or of possible blends, which can lead to systematic errors in lifetime measurements. However, rather few experimental lifetimes for Cd I and Cd II obtained using such techniques are, so far, available. Even the $4d^{10}5s5p\ ^1P^o_1$ resonance state of Cd I has not been investigated by selective excitation techniques.

Starting with the pioneering work of Zemansky [5] and of Koening and Ellett [6], the $5s5p\ ^1P^o_1$ and $5s5p\ ^3P^o_1$ levels of Cd I have been frequently investigated. In the early experimental work, the techniques adopted for lifetime measurements of low lying Cd I states included the Hanle effect method [7–10], the double resonance technique [11], the phase-shift approach [12,13], and the beam-foil method [14]. The lifetime of the $5s5d\ ^1D_2$state and the transition probabilities of the $5p\ ^1P^o_1$-$nd\ ^1D_2$ transitions have been measured in an argon inductivity coupled plasma [15]. Radiative lifetimes of levels belonging to the $5sns\ ^1S_0$, $nd\ ^1D_2$, $ns\ ^3S_1$, $np\ ^3P^o$, and $nd\ ^3D$ Cd I series have been investigated in a delayed-coincidence experiment with pulsed electron excitation [16,17]. A Hanle effect experiment with electron excitation was carried out by Frasinski and Duhnalik [18]. Only one measurement is available for the upper state of the resonance $np\ ^1P^o_1$ series—$10p\ ^1P^o_1$ [12].

In the only experiment carried out with selective excitation, the lifetimes of the $ns\ ^3S_1$and $nd\ ^3D$ excited states were investigated [19] while cascade-free measurements, obtained with an electron-photon coincidence technique, were performed for the 6, $7s\ ^1S_0$, and $5d\ ^1D_2$ levels [20].

Experimental transition probabilities in Cd I were obtained with an emission technique [21], eventually combined with the hook method [22]. Precise oscillator strength values of the $5s^2\ ^1S_0$-$5snp\ ^1P^o$ ($n=8-13$) transitions were measured by a magneto-optical rotation method [23] and the sum-frequency mixing in Cd vapor was considered for determination of matrix elements along the Cd I resonance series [24].

*Electronic address: kblagoev@issp.bas.bg

Theoretical work in the same atom includes the use of different methods such as the scaled Thomas-Fermi-Dirac approach [25], the Coulomb approximation [26], the extended Bates-Damgaard (nodal boundary condition) method [27], a relativistic "quantum orbital" [28], or a HF method [29]. Core-polarization effects were considered within the framework of a multiconfigurational Hartree-Fock method for *s-p* and *p-d* transitions [30]. The effect of configuration interaction and of core-polarization on the spin-allowed $5s^2\ ^1S_0$-$5s5p\ ^1P^o_1$ and spin-forbidden $5s^2\ ^1S_0$-$5s5p\ ^3P^o_1$ transitions were also investigated [31,32].

Radiative lifetimes of Cd II excited states have been measured using different experimental methods: beam-foil spectroscopy [14,33], the level-crossing approach [34–37], the phase-shift method with electron excitation [12], and the delayed-coincidence technique with electron excitation [16,38,39]. In these experiments, the low lying $5p\ ^2P^o_{1/2,3/2}$, $6s\ ^2S_{1/2}$, $5d\ ^2D_{3/2,5/2}$ and $4f\ ^2F^o$ levels have been investigated as well as the high members of the $ns\ ^2S_{1/2}$ and $nd\ ^2D_{3/2,5/2}$, series. Radiative lifetimes of the $5d^9 4s^2\ ^2D_{3/2,5/2}$ excited states have been determined with the delayed-coincidence [38], double resonance [40], and level-crossing [37] techniques. In all these experiments, nonselective excitation was considered and the results were suffering from eventual cascading problems. An electron-photon coincidence cascade-free experiment was carried out for the determination of the radiative lifetimes of the $5p\ ^2P^o_{1/2,3/2}$ excited states as well as for the $5d^9 4s^2\ ^2D_{3/2,5/2}$ Beutler levels [41]. In only one experiment, selective excitation on an ion beam was employed for radiative lifetime measurement of the $5p\ ^2P^o_{1/2,3/2}$ levels [33].

Theoretical approaches have been applied also in the case of Cd II. In particular, oscillator strengths have been calculated by a relativistic quantum defect orbital method for the $nd\ ^2D$-$5p\ ^2P^o_{1/2,3/2}$ (n=5–10) transitions [42]. A relativistic many-body, third order perturbation was used for calculation of radiative lifetimes of the $5p\ ^2P^o_{1/2,3/2}$ Cd II levels [43] and a core-polarization method was considered for calculation of $5s\ ^2S_{1/2}$-$np\ ^2P^o$ (n=5–7) transition probabilities [44]. Oscillator strengths of $5s\ ^2S_{1/2}$-$5p\ ^2P^o_{1/2,3/2}$ and of $5p\ ^2P^o_{1/2,3/2}$-$5d\ ^2D_{3/2,5/2}$ spectral lines were calculated with a relativistic Hartree-Fock approach taking core-polarization effects into account [45] while a Coulomb approximation and a quasiclassical approximation did allow the calculation of $ns\ ^2S_{1/2}$ (n=6-10) radiative lifetimes [39]. The Coulomb approximation was used [46], taking into account core polarization for calculation the oscillator strengths of resonance lines of Cd II.

From this survey of the available data for radiative lifetimes and transition probabilities of Cd I and Cd II excited states, it turns out that, although many lifetime measurements have been performed, only one paper has been published in which selective laser excitation was considered for triplet states of Cd I [19]. In addition, laser measurements were performed only for the $5p\ ^2P^o_{1/2,3/2}$ levels of Cd II (beam-laser method) [33]. As a consequence, the purpose of the present study is to obtain new accurate data for radiative lifetimes and transition probabilities of Cd I and Cd II excited states and to evaluate the accuracy of the data available in the literature. An additional purpose of the present work is to compare experimental work with theory for testing the adequacy of the theoretical models in relation with the increasing importance of the relativistic and core-polarization effects and with the progressive transition from *LS* and *jj* coupling in heavy elements. A theoretical approach has also been employed for generating transition probabilities or oscillator strengths from a combination of experimental lifetime measurements and theoretical branching fraction determinations. In addition, in Cd II these results have been compared with experimental values obtained considering branching fractions measured in a laser induced breakdown spectroscopy (LIBS) experiment.

In recent years, the development of laser spectroscopy techniques both in the time and wavelength domains has made laser measurements of radiative lifetimes in high-energy atomic or ionic levels feasible. In the current study, radiative lifetimes of excited states (up to 90 000 cm^{-1}) have been measured in Cd I and Cd II by time-resolved laser-induced fluorescence (LIF) using single or two-step excitations of atoms and ions produced in a laser-induced plasma. The results of this experiment are compared to a theoretical calculation of the lifetimes using multiconfigurational relativistic Hartree-Fock calculations, taking core-polarization effects into account. In addition, as transition probabilities and oscillator strengths available in the literature for Cd I and Cd II concern only a limited number of transitions, generally connecting levels of low excitation (see, e.g., Ref. [7]), transition probabilities and oscillator strengths have been deduced from the combination of experimental lifetimes and both theoretical and experimental branching fractions.

II. EXPERIMENT

A. Lifetime measurements

The ground states of Cd I and Cd II are $[Kr]4d^{10}5s^2\ ^1S_0$ and $[Kr]4d^{10}5s\ ^2S_{1/2}$, respectively. Radiative lifetimes of 11 levels of Cd I belonging to the $5snp$ (n=5), $5snd$ (n=6–9), $5sns$ (n=7,8) series, and of 5 levels of Cd II belonging to the $4d^{10}5p$, $4d^{10}6s$, and $4d^{10}5d$ configurations have been measured. The levels studied are shown in Fig. 1 with the relevant excitation schemes including single-step and two-step excitation processes.

The experimental setup used in the lifetime measurements is schematically shown in Fig. 2. Free neutral and singly ionized cadmium atoms were obtained by laser ablation. A 532-nm pulse, emitted from a Nd:YAG laser (Continuum Surelite) (laser A) with 10 ns pulse duration was focused onto a rotating cadmium foil located in a vacuum chamber with 10^{-6}–10^{-5} mbar background pressure. Plasma containing neutral, as well as ionized atoms in different ionization stages was produced by the laser pulse and expanded from the foil for subsequent laser excitation. The plasma cloud of cadmium was intersected at right angles by a linearly polarized, pulsed-laser beam tuned to a resonant transition of the upper state of interest. The $5p\ ^2P^o_{1/2,3/2}$ levels of Cd II and the $5s5p\ ^1P^o_1$ level of Cd I were populated from the ground state after single-photon excitation.

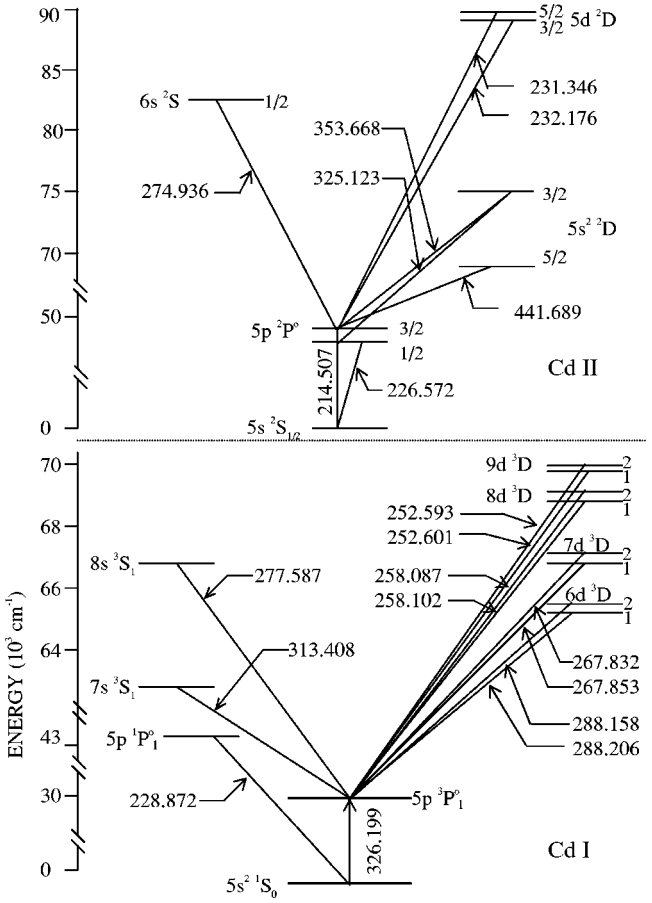

FIG. 1. Partial energy-level diagram of Cd I and Cd II showing the relevant excitation schemes. The wavelengths are given in nm.

A temporal compressor was used to shorten the laser pulse, emitted from a seeder injected Nd:YAG laser (Continuum NY-82) (laser B), with 8 ns pulse duration and 400 mJ pulse energy at 532 nm. The design and construction of the Stimulated Brillouin Scattering (SBS) compressor, similar to the one described in Ref. [47], is shown in Fig. 3. The pulse duration of the output from the SBS temporal compressor was approximately 1 ns and the loss in pulse energy was about 50%. The compressed pulse was used to pump a dye laser (Continuum Nd-60), operated with a DCM dye. The radiation from the dye laser was frequency doubled in a KDP crystal and then mixed with the fundamental frequency in a BBO crystal, to generate the third harmonic of the dye laser frequency. The spectral range was expanded by focusing the second or the third harmonic of the dye laser beam into a H_2 cell at 10 bar, in which different orders of stimulated Stokes scattering were obtained. Depending on the excitation requirement, the appropriate beam component was selected with a CaF_2 Pellin-Broca prism.

For the $5snd\,^3D_{1,2}$ ($n=6-9$) and $5sns\,^3S_1$ ($n=7,8$) series of Cd I, and $6s\,^2S_{1/2}$ and $5d\,^2D_{3/2,5/2}$ levels of Cd II, two-step excitation processes have been applied. In this case, the compressed-pulse laser system was used as the second-step excitation. Another laser system with 8 ns pulse duration was employed as the first-step excitation source.

A second Continuum NY-82 Nd:YAG laser (laser C) was used to pump another Continuum Nd-60 dye laser, which was also operated with a DCM dye. For Cd I measurements, the dye laser was tuned to 652.22 nm. The second harmonic of the dye radiation was obtained in a KDP crystal and was used in the first step to excite the $5p\,^3P^o_1$ state at 30656.130 cm^{-1}. For the Cd II experiment, the $5p\,^2P^o_{3/2}$ level at 49355.04 cm^{-1} was employed as the intermediate state. The dye laser was tuned to 643.34 nm, and then its third harmonic, produced in a BBO crystal, could be utilizd to reach the level for the first step excitation. All three Nd:YAG lasers (A, B, C) used in this experiment were externally triggered by a digital pulse generator (Stanford Research Systems Model DG535), which was used for temporal synchronization of the two laser pulses for the first and second step excitations and also for a free variation of the delay time between the excitation and ablation pulses.

Photons emitted in the spontaneous decay of the excited levels were recorded by a detection system, which included a fused-silica lens, a 1/8 m monochromator (resolution 6.4 nm/mm), and a Hamamatsu R1564U photomultiplier (200 ps rise time). The transient signals were captured and averaged by a Tektronix DSA 602 digital oscilloscope. The decay curves were obtained by averaging the signals from about 1000–2000 pulses. Approximately 10–30 curves were recorded for each level under study.

For the $5snd\,^3D_{1,2}$ ($n=6-9$) and $5sns\,^3S_1$ ($n=7,8$) long-lived levels of Cd I ($\tau>15$ ns), the lifetimes were evaluated using a least-square exponential fitting procedure (see Fig. 4). For the other short-lived excited states, the temporal shape of the exciting laser pulses was recorded after the ablation beam was blocked. The decay curves were treated by deconvolution of the observed signal and of the laser pulse (see Fig. 5).

Measurements under different conditions were performed to avoid systematic errors. The occasional signal contribution due to the scattered light from the excitation laser was eliminated by subtraction of the signal observed without an ablation pulse.

No observable effects of quantum beats due to the laboratory magnetic field were observed in the experiment. In order to remove any possible influence on the longer lifetimes a magnetic field of about 100 Gauss, provided by a pair of Helmholtz coils, was also added.

The possible influence of the radiation trapping on the signal from the resonance $5s5p\,^1P^o_1$ level in Cd I and from the $5p\,^2P^o_{1/2,3/2}$ levels in Cd II was investigated by considering small delay times between the ablation and excitation pulses. When the delay time is short, the radiation trapping can possibly influence the lifetime values. When the delay time gets longer, the concentration of atoms and ions decreases and the radiation trapping effects can be neglected. In the present experiment, for the $5p\,^1P^o_1$ level of Cd I, the measurements were carried out at delay times $t=30-40$ μs and, for the levels $4p\,^2P_{1/2,3/2}$ of Cd II, at $t=6-12$ μs. At these values of the delay, no effect of radiation trapping was observed. The dependence of lifetime values on the delay time between ablation and excitation laser pulses was studied in Ref. [49]. The possible influence of saturation of the transitions was also checked by carrying out the measurements at different energies of the excitation laser pulses.

All experimental lifetime results are summarized in Tables I–IV with statistical error bars. We give also, in the

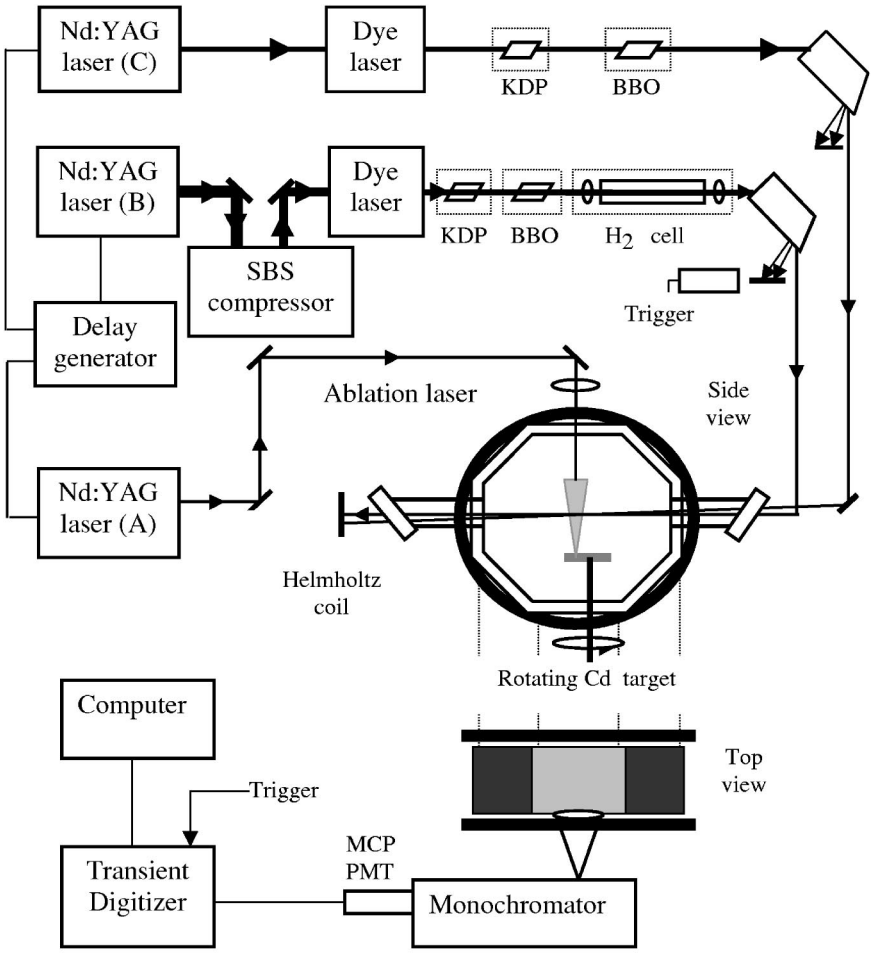

FIG. 2. Experimental setup used for the lifetime measurements (see the text).

same tables, the theoretical lifetime values obtained according to the procedure described below.

B. Transition probability determination

A plasma produced by laser ablation was employed as a source of Cd II ions. A focused Nd:YAG laser beam was used to generate the plasma on the surface of a cadmium target in a controlled argon atmosphere (~8 Torr). A 1064 nm Nd:YAG laser generated 240 mJ pulses of 7 ns duration at a frequency of 20 Hz. The light emitted by the laser-produced plasma was focused on the input slit of 1-m grating Czerny-Turner monochromator (resolution 0.03 nm). The spectra were recorded by a time-resolved optical multichannel analyzer (OMA III, EG&G), that allowed recording of spectral regions at different delays after the laser pulse and during a selected time interval (Fig. 6).

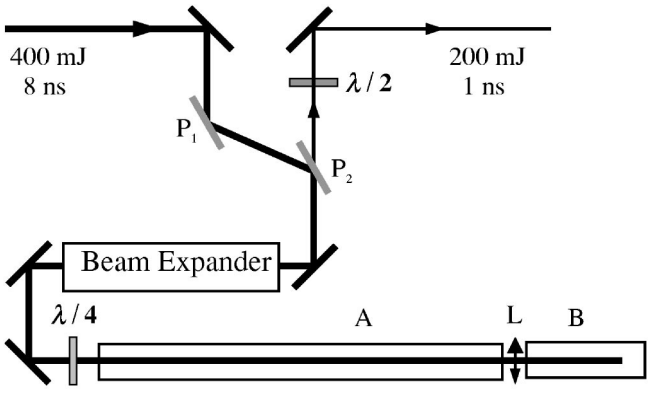

FIG. 3. Stimulated Brillouin scattering (SBS) compressor. λ/2 (half-wave) and λ/4 (quarter-wave) retarding plates are inserted. P_1 and P_2 are plate polarizers placed at the Brewster angle, L is a lens of 15 cm focal length, A is a 150 cm and B a 30 cm glass tube with pure water.

The calibration of the spectral response of the experimental system was made, before the experiment, using a standard deuterium lamp in the wavelength range 200 to 400 nm, and a standard tungsten lamp in the range 350 to 600 nm. The final calibration was a result of overlapping of several joint regions of the deuterium and tungsten lamps employing a least-square fitting procedure. The calibration of the system was also checked by measurements of branching fractions of well known Ar I and Ar II spectral lines. The two types of calibration were in agreement within an error limit of 5%. In order to check the time evolution of the response of the OMA photodiode array, the calibration of the system was repeated regularly and was compared with the response of the photodiode array using the 431.6 nm Kr I spectral line, which is measured by different channels of the detector (50 channel steps in a 1024 array). The difference, due to time

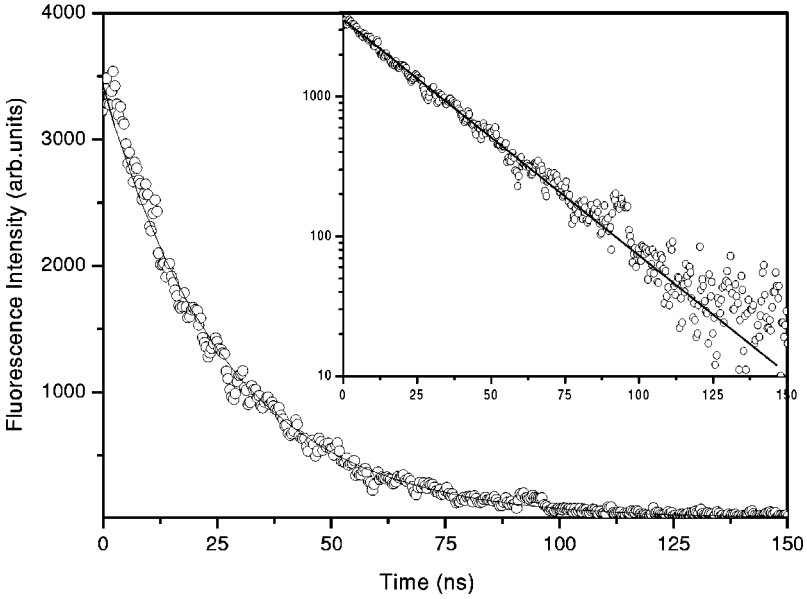

FIG. 4. Typical experimental curve (dots) from the $7s\ ^3S_1$ state of Cd I, with an exponential fit (solid line) that gives a lifetime of 24.4 ns. The inset shows the same data in a semilogarithmic representation.

evolution of the calibration, is around 2%. The error due to the calibration is estimated around 6%.

Detection was made in synchronization with the electronic trigger of the *Q*-switched laser. During data acquisition, a subtraction was made of the background.

The method is based on the fact that there is an optimized delay time after laser ablation for recording the spectrum of the selected ion. In this way, the measurements are made at several delay times after the laser pulse, more precisely after 0.1, 0.2, 0.3, and 0.5 μs delay time. The measurements of branching ratios for the determination of transition probabilities have been made on the spectra obtained at a delay of 0.3 μs because the lines were better resolved and narrower than those obtained with shorter delays, on the one hand, and were more intense than those corresponding to longer delays, on the other hand (Fig. 7). The measured branching fractions did not depend on the delay time.

The spectra were stored in a computer and treated by a software which is able to separate close or overlapping lines and to determine their relative intensities. The relative intensities were obtained by a fitting procedure based on the use of Voigt profiles, after subtraction of the background. In the present experiment, there is no overlapping of the investigated spectral lines with other spectral lines of cadmium ions or of Ar I, Ar II spectral lines. The final intensity of each line was the average of eight different measurements. To prevent self-absorption effects, several alloys of cadmium and zinc have been used instead of pure cadmium. The content of cadmium in these alloys ranged from 5 to 10 % and it was verified that the branching ratios were not depending upon concentration. Using these alloys, it turned out that the spectral line of Cd II at 226.5 nm ($5s\ ^2S_{1/2}$-$5p\ ^2P^o_{1/2}$) was blended with the spectral line of Zn II at 226.55 nm. In this case, for estimating the real intensity of the 226.50 nm line, the second order spectrum was used.

In a first step, relative experimental transition probabilities were obtained and then, in a second step, they were put on an absolute scale using the measured branching ratios and

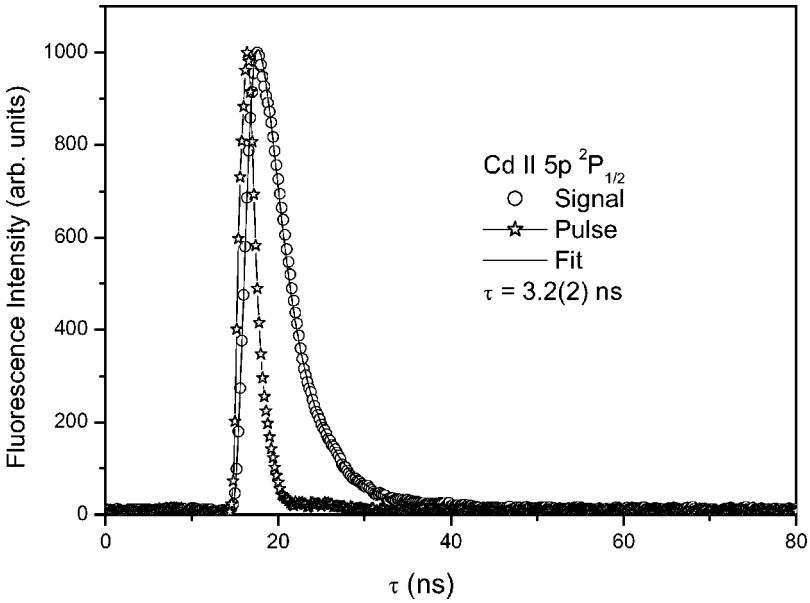

FIG. 5. A typical decay curve for the $5p\ ^2P^o_{1/2}$ state of Cd II, with a convolution fit.

TABLE I. Radiative lifetimes of Cd I (ns).

		This work			Previous works	
			Theory			
State	E (cm^{-1})	Experiment	A	B	Experiment	Theory
$5p\ ^1P^o_1$	43692.47	1.75(0.2)	1.37	1.39	1.99,[a] 1.66(0.05),[b] 2.1(0.3),[c] 1.9(0.15),[d] 2.1[e]	1.43[f,g]
$7s\ ^3S_1$	62563.46	24.4(1.6)	19.53	15.91	18.5(0.9),[h] 13.7(1.5),[d] 25(2),[i] 22.4(1.0),[j] 29.9(4.5)[k]	28.9,[j] 41.5,[k] 21.7,[f] 28.5,[g]
$8s\ ^3S_1$	66680.92	50.8(0.8)	40.95	32.73	48.1(1.5),[i] 48.1(2.5)[j]	66.3[j]
$6d\ ^3D_1$	65353.5	17.3(0.4)	14.28	12.86	15.5(1.3),[h] 15.6(0.8)[j]	12.7,[j] 13.4,[f] 12.7[g]
$6d\ ^3D_2$	65359.3	18.1(1.0)	14.89	13.30	15.2(0.5),[h] 15.8(0.6)[j]	13.3,[j] 14.1,[f] 13.3[g]
$6d\ ^3D_j$					17.4(1.9),[i] 11.5(1.5),[d] 18.7(2.4)[k]	17.1[k]
$7d\ ^3D_1$	67990.1	32.1(3.0)	30.10	26.71	19(2),[h] 30.2(2)[j]	28.1[j]
$7d\ ^3D_2$	67992.9	33.4(0.8)	31.26	27.53	24(2),[h] 30.5(1.5)[j]	29.2[j]
$7d\ ^3D_j$					32.7(2.2),[i] 23(3)[d]	
$8d\ ^3D_1$	69400.5	53(5)	57.36	49.67		
$8d\ ^3D_2$	69402.8	54.7(1.0)	59.43	51.10	53.5(2.5)[j]	50.9[j]
$8d\ ^3D_j$					56.3(4.2)[i]	
$9d\ ^3D_1$	70244.2	89(9)	105.8	83.48		
$9d\ ^3D_2$	70245.5	91(9)	109.53	85.76		
$9d\ ^3D_j$					85.1(4.7)[i]	

[a]Hanle [5].
[b]Hanle [7].
[c]Phase-shift method [12].
[d]Beam-foil [14].
[e]Phase shift [13].
[f]Quasirelativistic Hartree-Fock.
[g]Coulomb approximation [30].
[h]Hanle [8].
[i]Delayed coincidence method [17].
[j]Delayed coincidence method with laser excitation, Coulomb approximation [19].
[k]Delayed coincidence method, Coulomb approximation [16].

the radiative lifetimes of the upper states. These data are presented as the column Exp. 1 in Table IV. The total errors were determined from the radiative lifetimes errors, from the uncertainties affecting the calibration (6%) and from statistical errors, which, for the different lines, were ranging from 5.9 to 10 %. The transition probabilities of the lines emitted from the $4d^8 5s^2\ ^2D_{3/2}$ level were normalized using a theoretical estimate of the radiative lifetime; the error shown for this state in column Exp. 1 of Table IV is resulting from calibration and statistical errors.

Assuming LTE and a value of the electron density, one can estimate the self-absorption of the emitting plasma, which can influence measured branching ratios. The electron density was estimated from the Stark broadening of the Cd II line at 226.502 nm. The value of $N_e = 1.1 \times 10^{17}$ cm^{-3} has been deduced using the Stark broadening parameter [48], which is $\omega = 0.0061$ nm (FWHM). This value is sufficient to assume that the LTE assumption is justified for the population of the investigated levels according to the criterion of Ref. [50]:

$$N_e\ (\mathrm{cm}^{-3}) \geqslant 1.6 \times 10^{12} [T(K)]^{1/2} [\Delta E(\mathrm{eV})]^3,$$

where N_e is the electron number density, ΔE is the energy difference between both configurations, and T is the plasma temperature. The plasma temperature was deduced by assuming local thermodynamic equilibrium (LTE). This temperature was determined from the slope of a Boltzmann plot of the line intensities of transitions with known transition probabilities. The temperature under the present experimental conditions was determined to be 15500 ± 1800 K. In our case $\Delta E = 2.6$ eV and the lower limit given by this expression is $N_e = 3.5 \times 10^{15}$ cm^{-3}. The absorption coefficient was calculated from the Cd II density and from the populations of Cd II excited states. Integrating along the line profiles, it is assumed that the plasma is optically thin when the self-absorption is less than 3% [51]. In the present experiment, for a plasma thickness of 1 mm, the line intensity absorption, integrated along the line profile, was less than 2.4% for the line 231.2 nm of Cd II. For the other lines, this absorption coefficient was even lower.

The transition probabilities can also be determined from comparison of the line intensities with those with known transition probabilities and plasma temperature in LTE conditions. In particular, the transition probabilities of the lines emitted from the $5p\ ^2P^o_{1/2,3/2}$, $5d\ ^2D_{5/2}$, and $4d^9 5s^2\ ^2D_{5/2}$ levels (at 214.4, 226.5, 231.2, and 441.6 nm; see Fig. 1, Table IV) were calculated in this way, as well. The temperature was determined from the slope of a Boltzmann plot. The experimental errors in this case have been estimated to reach 12%, and were obtained as the sum of the above mentioned uncertainties and of an uncertainty resulting from the temperature determination (10%). These results are presented in Table IV in the column Exp. 2. Results of both experiments agree in the error limit.

TABLE II. Cd I: oscillator strengths and transition probabilities ($\log gf > -2.0$) for the transitions depopulating the levels measured in the present work (the intercombination lines are not included). We give the HFR results (calculation B) and the values normalized with the experimental lifetimes as measured in the present work.

	This work					Previous works ($\log gf$)	
	HFR			NORM			
Transition	$\log gf$	gA (s^{-1})	CF	$\log gf$	gA (s^{-1})	Experiment	Theory
$5s^2\ ^1S_0$-$5p\ ^1P_1$	0.22	2.15×10^9	0.582	0.11	1.69×10^9	0.34,[d] 0.19,[h] 0.29,[g] 0.13[i]	
$5p\ ^3P^o_0$-$7s\ ^3S_1$	1.61	1.76×10^7	−0.215	−1.80	1.15×10^7	−1.26[f]	−1.82,[a] −1.83,[b] −1.77,[c] −1.76,[d] −1.70[e]
$5p\ ^3P^o_1$-$7s\ ^3S_1$	−1.14	5.10×10^7	−0.214	−1.33	3.33×10^7	−0.62[f]	−1.35,[a] −1.35,[b] −1.29,[c] −1.29,[d] −1.22[e]
$5p\ ^3P^o_2$-$7s\ ^3S_1$	−0.93	7.95×10^7	−0.211	−1.12	5.18×10^7	−0.38[f] −1.12,[a] −1.12,[b] −1.07,[c] −1.09,[d] −1.02[e]	
$6p\ ^3P^o_0$-$7s\ ^3S_1$	−0.44	4.94×10^6	−0.725	−0.63	3.22×10^6		−0.56,[d] −0.44[c]
$6p\ ^3P^o_1$-$7s\ ^3S_1$	0.03	1.41×10^7	−0.724	−0.16	9.22×10^6		−0.09,[d] −0.98[e]
$6p\ ^3P^o_2$-$7s\ ^3S_1$	0.24	2.13×10^7	−0.721	0.05	1.39×10^7		0.13,[d] 0.23[e]
$5p\ ^3P^o_0$-$6d\ ^3D_1$	−0.86	1.15×10^8	−0.320	−0.99	8.57×10^7	−0.40,[f] −0.90,[b] −0.87[e]	
$5p\ ^3P^o_1$-$6d\ ^3D_1$	−0.99	8.37×10^7	0.317	−1.12	6.22×10^7	−0.44[f]	−1.02,[b] −1.11,[c] −1.00[e]
$6p\ ^3P^o_0$-$6d\ ^3D_1$	−0.32	1.63×10^7	−0.580	−0.45	1.21×10^7		−0.30[e]
$6p\ ^3P^o_1$-$6d\ ^3D_1$	−0.45	1.19×10^7	0.579	−0.58	8.81×10^6		−0.44[e]
$6p\ ^3P^o_2$-$6d\ ^3D_1$	−1.64	7.41×10^5	−0.574	−1.77	5.51×10^5	−1.60[e]	
$7p\ ^3P^o_0$-$6d\ ^3D_1$	−0.30	1.08×10^5	0.915	0.43	7.99×10^4		
$7p\ ^3P^o_1$-$6d\ ^3D_1$	−0.45	6.99×10^4	−0.914	−0.58	5.19×10^4		
$7p\ ^3P^o_2$-$6d\ ^3D_1$	−1.67	3.33×10^3	0.914	−1.80	2.48×10^3		
$5p\ ^3P^o_1$-$6d\ ^3D_2$	−0.52	2.51×10^8	−0.317	−0.65	1.84×10^8	−0.002[f]	−0.54,[b] −0.53[e]
$5p\ ^3P^o_2$-$6d\ ^3D_2$	−1.01	7.80×10^7	0.312	−1.14	5.73×10^7	−0.42[f]	−1.01,[b] −1.10,[c] −1.02[e]
$6p\ ^3P^o_1$-$6d\ ^3D_2$	0.02	3.55×10^7	−0.577	−0.11	2.61×10^7		0.03[e]
$6p\ ^3P^o_2$-$6d\ ^3D_2$	−0.46	1.11×10^7	0.574	−0.59	8.17×10^6		−0.45[e]
$7p\ ^3P^o_1$-$6d\ ^3D_2$	0.03	2.12×10^5	0.913	−0.10	1.56×10^5		
$7p\ ^3P^o_2$-$6d\ ^3D_2$	−0.49	5.08×10^4	−0.914	−0.62	3.73×10^4		
$5p\ ^3P^o_1$-$8s\ ^3S_1$	−1.59	2.32×10^7	−0.114	−1.77	1.52×10^7	−1.20[f]	−1.75,[c] −1.74[d]
$5p\ ^3P^o_2$-$8s\ ^3S_1$	−1.37	3.65×10^7	−0.112	−1.55	2.39×10^7	−0.98[f]	−1.54,[c] −1.52[d]
$6p\ ^3P^o_0$-$8s\ ^3S_1$	−1.59	1.27×10^6	−0.246	−1.77	8.31×10^5		−1.66[d]
$6p\ ^3P^o_1$-$8s\ ^3S_1$	−1.12	3.71×10^6	−0.245	−1.30	2.43×10^6		−1.18[d]
$6p\ ^3P^o_2$-$8s\ ^3S_1$	−0.90	5.91×10^6	−0.243	−1.08	3.87×10^6		−0.96[d]
$7p\ ^3P^o_0$-$8s\ ^3S_1$	−0.24	1.59×10^6	−0.775	−0.42	1.04×10^6		−0.37[d]
$7p\ ^3P^o_1$-$8s\ ^3S_1$	0.24	4.58×10^6	−0.774	0.06	3.00×10^6		0.09[d]
$7p\ ^3P^o_2$-$8s\ ^3S_1$	0.45	7.00×10^6	−0.772	0.27	4.58×10^6		0.30[d]
$5p\ ^3P^o_0$−$7d\ ^3D_1$	−1.28	5.15×10^7	−0.195	−1.36	4.28×10^7	−0.92[f]	−1.36[c]
$5p\ ^3P^o_1$-$7d\ ^3D_1$	−1.41	3.74×10^7	0.193	−1.49	3.11×10^7		−1.48[c]
$6p\ ^3P^o_0$-$7d\ ^3D_1$	−0.90	8.11×10^6	−0.366	−0.98	6.75×10^6		
$6p\ ^3P^o_1$-$7d\ ^3D_1$	−1.03	5.94×10^6	0.365	−1.11	4.94×10^6		
$7p\ ^3P^o_0$-$7d\ ^3D_1$	−0.31	3.45×10^6	−0.565	−0.39	2.87×10^6		
$7p\ ^3P^o_1$-$7d\ ^3D_1$	−0.44	2.52×10^6	0.564	−0.52	2.10×10^6		
$7p\ ^3P^o_2$-$7d\ ^3D_1$	−1.63	1.59×10^5	−0.560	−1.71	1.32×10^5		
$4f\ ^3F^o_2$-$7d\ ^3D_1$	−1.37	2.16×10^5	−0.479	−1.45	1.80×10^5		
$8p\ ^3P^o_0$-$7d\ ^3D_1$	0.03	1.42×10^5	0.930	-0.05	1.18×10^5		
$8p\ ^3P^o_1$-$7d\ ^3D_1$	−0.11	9.68×10^4	−0.930	−0.19	8.05×10^4		
$8p\ ^3P^o_2$-$7d\ ^3D_1$	−1.31	5.26×10^3	0.930	−1.39	4.38×10^3		
$5f\ ^3F^o_2$−$7d\ ^3D_1$	0.05	3.96×10^4	0.953	−0.03	3.30×10^4		
$5p\ ^3P^o_1$-$7d\ ^3D_2$	−0.93	1.12×10^8	−0.193	−1.01	9.33×10^7	−1.00[c]	
$5p\ ^3P^o_2$-$7d\ ^3D_2$	−1.42	3.51×10^7	0.189	−1.50	2.89×10^7	−1.46[c]	

TABLE II. (*Continued.*)

	This work					Previous works (log gf)	
	HFR			NORM			
Transition	log gf	gA (s^{-1})	CF	log gf	gA (s^{-1})	Experiment	Theory
$6p\ ^3P^o_1$-$7d\ ^3D_2$	−0.56	1.78×10^7	−0.364	−0.64	1.47×10^7		
$6p\ ^3P^o_2$-$7d\ ^3D_2$	−1.04	5.69×10^6	0.362	−1.12	4.69×10^6		
$7p\ ^3P^o_1$-$7d\ ^3D_2$	0.03	7.55×10^6	−0.562	−0.05	6.22×10^6		
$7p\ ^3P^o_2$-$7d\ ^3D_2$	−0.45	2.39×10^6	0.560	−0.53	1.97×10^6		
$4f\ ^3F^o_3$−$7d\ ^3D_2$	−1.26	2.78×10^5	−0.481	−1.34	2.30×10^5		
$8p\ ^3P^o_1$-$7d\ ^3D_2$	0.37	2.93×10^5	0.929	0.29	2.41×10^5		
$8p\ ^3P^o_2$-$7d\ ^3D_2$	−0.14	7.97×10^4	−0.930	−0.22	6.57×10^4		
$5f\ ^3F^o_2$-$7d\ ^3D_2$	−0.68	7.47×10^3	0.953	−0.76	6.15×10^3		
$5f\ ^3F^o_3$−$7d\ ^3D_2$	0.17	5.23×10^4	0.953	0.25	4.31×10^4		
$5p\ ^3P^o_0$-$8d\ ^3D_1$	−1.61	2.60×10^7	−0.119	−1.64	2.44×10^7	−1.64[c]	
$5p\ ^3P^o_1$-$8d\ ^3D_1$	−1.74	1.89×10^7	0.118	−1.77	1.77×10^7	−1.74[c]	
$6p\ ^3P^o_0$-$8d\ ^3D_1$	−1.29	4.35×10^6	−0.246	−1.32	4.08×10^6		
$6p\ ^3P^o_1$-$8d\ ^3D_1$	−1.42	3.20×10^6	0.245	−1.45	2.99×10^6		
$7p\ ^3P^o_0$-$8d\ ^3D_1$	−0.88	1.93×10^6	−0.373	−0.91	1.80×10^6		
$7p\ ^3P^o_1$-$8d\ ^3D_1$	−1.01	1.42×10^6	0.372	−1.04	1.33×10^6		
$8p\ ^3P^o_0$-$8d\ ^3D_1$	−0.28	1.25×10^6	−0.552	−0.31	1.17×10^6		
$8p\ ^3P^o_1$-$8d\ ^3D_1$	−0.40	9.13×10^5	0.551	−0.43	8.55×10^5		
$8p\ ^3P^o_2$-$8d\ ^3D_1$	−1.59	5.80×10^4	−0.548	−1.62	5.44×10^4		
$5f\ ^3F^o_2$-$8d\ ^3D_1$	−0.93	2.16×10^5	−0.529	−0.96	2.02×10^5		
$9p\ ^3P^o_0$-$8d\ ^3D_1$	0.32	2.19×10^5	0.939	0.29	2.05×10^5		
$9p\ ^3P^o_1$-$8d\ ^3D_1$	0.19	1.55×10^5	−0.939	0.16	1.45×10^5		
$9p\ ^3P^o_2$-$8d\ ^3D_1$	−1.01	9.09×10^3	0.939	−1.04	8.52×10^3		
$5p\ ^3P^o_1$−$8d\ ^3D_2$	−1.26	5.68×10^7	−0.117	−1.29	5.28×10^7	−1.27[c]	
$5p\ ^3P^o_2$-$8d\ ^3D_2$	−1.75	1.77×10^7	0.114	−1.78	1.65×10^7	−1.70[c]	
$6p\ ^3P^o_1$-$8d\ ^3D_2$	−0.94	9.57×10^6	−0.244	−0.97	8.90×10^6		
$6p\ ^3P^o_2$−$8d\ ^3D_2$	−1.43	3.08×10^6	0.242	−1.46	2.86×10^6		
$7p\ ^3P^o_1$−$8d\ ^3D_2$	−0.54	4.24×10^6	−0.371	−0.57	3.94×10^6		
$7p\ ^3P^o_2$−$8d\ ^3D_2$	−1.02	1.37×10^6	0.369	−1.05	1.27×10^6		
$8p\ ^3P^o_1$-$8d\ ^3D_2$	0.07	2.74×10^6	−0.549	0.04	2.54×10^6		
$8p\ ^3P^o_2$-$8d\ ^3D_2$	−0.41	8.71×10^5	0.548	−0.44	8.10×10^5		
$5f\ ^3F^o_2$-$8d\ ^3D_2$	−1.66	4.00×10^4	−0.529	−1.69	3.72×10^4		
$5f\ ^3F^o_3$-$8d\ ^3D_2$	−0.82	2.82×10^5	−0.530	−0.85	2.62×10^5		
$9p\ ^3P^o_1$-$8d\ ^3D_2$	0.66	4.67×10^5	0.937	0.63	4.34×10^5		
$9p\ ^3P^o_2$−$8d\ ^3D_2$	0.17	1.37×10^5	−0.939	0.14	1.27×10^5		
$5p\ ^3P^o_0$-$9d\ ^3D_1$	−1.88	1.45×10^7	−0.076	−1.91	1.36×10^7	−1.85[c]	
$6p\ ^3P^o_0$-$9d\ ^3D_1$	−1.60	2.49×10^6	−0.167	−1.63	2.33×10^6		
$6p\ ^3P^o_1$-$9d\ ^3D_1$	−1.73	1.83×10^6	0.166	−1.76	1.72×10^6		
$7p\ ^3P^o_0$-$9d\ ^3D_1$	−1.26	1.13×10^6	−0.263	−1.29	1.06×10^6		
$7p\ ^3P^o_1$-$9d\ ^3D_1$	−1.39	8.33×10^5	0.262	−1.42	7.81×10^5		
$8p\ ^3P^o_0$-$9d\ ^3D_1$	−0.85	6.98×10^5	−0.373	−0.88	6.55×10^5		
$8p\ ^3P^o_1$-$9d\ ^3D_1$	−0.98	5.14×10^5	0.372	−1.01	4.82×10^5		
$5f\ ^3F^o_2$−$9d\ ^3D_1$	−1.71	8.27×10^4	−0.284	−1.74	7.76×10^4		
$9p\ ^3P^o_0$-$9d\ ^3D_1$	−0.21	6.34×10^5	−0.544	−0.24	5.95×10^5		
$9p\ ^3P^o_1$-$9d\ ^3D_1$	−0.34	4.66×10^5	0.544	−0.37	4.37×10^5		
$9p\ ^3P^o_2$-$9d\ ^3D_1$	−1.53	2.98×10^4	−0.541	−1.56	2.80×10^4		

TABLE II. (*Continued.*)

	This work					Previous works ($\log gf$)	
	HFR			NORM			
Transition	$\log gf$	gA (s^{-1})	CF	$\log gf$	gA (s^{-1})	Experiment	Theory
$10p\ ^3P^o_0$-$9d\ ^3D_1$	0.58	3.51×10^5	0.944	0.55	3.29×10^5		
$10p\ ^3P^o_1$-$9d\ ^3D_1$	0.45	2.53×10^5	−0.944	0.42	2.37×10^5		
$10p\ ^3P^o_2$-$9d\ ^3D_1$	−0.74	1.55×10^4	0.944	−0.77	1.45×10^4		
$5p\ ^3P^o_1$-$9d\ ^3D_2$	−1.53	3.17×10^7	−0.075	−1.55	3.05×10^7	−1.52[c]	
$6p\ ^3P^o_1$-$9d\ ^3D_2$	−1.25	5.48×10^6	−0.165	−1.27	5.28×10^6		
$6p\ ^3P^o_2$-$9d\ ^3D_2$	−1.73	1.77×10^6	0.164	−1.75	1.70×10^6		
$7p\ ^3P^o_1$-$9d\ ^3D_2$	−0.91	2.50×10^6	−0.261	−0.93	2.40×10^6		
$7p\ ^3P^o_2$-$9d\ ^3D_2$	−1.39	8.08×10^5	0.260	−1.41	7.78×10^5		
$8p\ ^3P^o_1$-$9d\ ^3D_2$	−0.50	1.54×10^6	−0.371	−0.52	1.49×10^6		
$8p\ ^3P^o_2$-$9d\ ^3D_2$	−0.98	4.99×10^5	0.370	−1.00	4.81×10^5		
$5f\ ^3F^o_3$-$9d\ ^3D_2$	−1.59	1.08×10^5	−0.285	−1.61	1.04×10^5		
$9p\ ^3P^o_1$-$9d\ ^3D_2$	0.13	1.40×10^6	−0.542	0.11	1.35×10^6		
$9p\ ^3P^o_2$-$9d\ ^3D_2$	−0.35	4.48×10^5	0.541	−0.37	4.32×10^5		
$10p\ ^3P^o_2$-$9d\ ^3D_2$	0.43	2.34×10^5	−0.944	0.41	2.25×10^5		

[a]Single-configuration Coulomb approximation [26].
[b]Semiempirical calculations [29].
[c]Relativistic quantum defect orbital calculations with CP [28].
[d]Intermediate coupling and scaled Thomas-Fermi-Dirac wave functions [25].
[e]Quasirelativistic Hartree-Fock with relativistic corrections method [30].
[f]Experiment-arc discharge in Cd vapor [21].
[g]Nodal boundary condition method [27].
[h]*Ab initio* calculations with semiempirical corrections [31].
[i]Multiconfiguration relativistic Hartree-Fock with intravalence correlation and CP [32].

III. THEORY

A. HFR calculations in Cd I

As noted above the ground state configuration of Cd I is $4d^{10}5s^2\ ^1S_0$. The energy levels reported in the NBS compilation [52], based on early analyses of this spectrum, are generally given with one decimal and it is claimed in the introduction to the NBS tables that "the accuracy of the present data could be greatly improved with modern observations, particularly in the infrared region." Below the first ionization limit, the levels quoted belong to the configurations $5s^2$, $5sns$ ($n=6-16$), $5snp$ ($n=5-11$), $5snd$ ($n=5-19$), and $5snf$ ($n=4,5$). Above the ionization limit, a number of levels belonging to $4d^{10}5p^2$ and $4d^95s^2nl$ ($n\leqslant14, l=p,f$) have also been determined experimentally. In the present calculations and, particularly in the least-squares fitting procedure hereafter described, we used only the levels given below the ionization limit.

The calculations were performed in the framework of the pseudorelativistic Hartree-Fock (HFR) method with help of the Cowan suite of computer codes [53] modified for consideration of core-polarization (CP) effects (see, e.g., Ref. [54]). This approach, although based on the Schrödinger equation, does include the most important relativistic effects such as the mass-velocity corrections and Darwin contribution.

In the first calculation (calculation A), made with help of the Cowan suite of computer codes [53] modified for consideration of core-polarization (CP) effects (see, e.g., Ref. [54]), the following configurations are considered along the Rydberg series:

$$4d^{10}5s^2 + 4d^{10}5sns\ (n=6-12) + 4d^{10}5snd\ (n=5-12) + 4d^{10}5sng\ (n=5-12) + 4d^{10}5sni\ (n=7-12)$$

and

$$4d^{10}5snp\ (n=5-12) + 4d^{10}5snf\ (n=4-12) + 4d^{10}5snh\ (n=6-12).$$

CP effects, which are expected to be important in this heavy neutral element, were introduced in the calculations in the following way. The static dipole polarizability of Cd II is that computed by Fraga *et al.* [55], i.e., $\alpha_d=23.619\ a_0^3$, where a_0 is the value of the first Bohr orbit of the hydrogen atom. The cutoff radius r_c was chosen equal to 2.779 a_0 and corresponds to the mean value $\langle r\rangle$ of the outermost orbital $5s$ in the configuration $4d^{10}5s$. As we were interested in Rydberg states, the configuration sets were extended to high members of the series (in fact up to $n=12$).

The calculated eigenvalues of the Hamiltonian were optimized to the observed energy levels via a least-squares fitting procedure. In fact, all the levels up to $n=12$, below the ionization limit, were included in the fitting procedure.

TABLE III. Radiative lifetimes of Cd II (ns).

	This work				Previous works	
		Theory				
State	Experiment	C	D	E	Experiment	Theory
$6s\ ^2S_{1/2}$	2.1(2)	1.79	1.90		2.2(2),[a] 5.7(9)[b]	2.2[k]
$5p\ ^2P^o_{1/2}$	3.2(2)	2.92	2.99		3.11(4),[c] 4.8(1.0),[d] 3.5(2),[c] 3.05(13)[f]	2.74,[f] 3.10[l]
$5p\ ^2P^o_{3/2}$	2.5(3)	2.50	2.55		2.77(7),[c] 3.4(7),[d] 3.5(2),[e] 3.0(2),[g] 2.70(25)[f]	2.3,[f] 2.84[l]
$5p\ ^2P^o_j$					3.4(4),[a] 3.55(15),[h] 2.86(25)[i]	
$5d\ ^2D_{3/2}$	1.8(2)	1.23	1.32		2.0(1),[g] 1.79(11)[m]	
$5d\ ^2D_{5/2}$	1.7(2)	1.40	1.50		1.85(15)[m]	
$5d\ ^2D_j$					2.6(3),[a] 2.3(1)[g]	
$5s^2\ ^2D_{3/2}$				222	460(90),[d] 340(30),[g] 280(14)[j]	
$5s^2\ ^2D_{5/2}$				588	830(80),[g] 800(40)[j]	

[a]Beam-foil [14].
[b]Delayed coincidence method [16].
[c]Beam-laser, beam foil (ANDC) [33].
[d]Phase-shift method [12].
[e]Delayed coincidence method [38].
[f]Hanle theory [36].
[g]Hanle [34].
[h]Electron-photon delayed coincidence method [41].
[i]Hanle [35].
[j]Hanle [37].
[k]Quasiclassical theory [39].
[l]Many-body, third order perturbation theory [43].
[m]Beam-foil, multiexponential analysis [33].

The scaling factors of the F^k, G^k, and R^k integrals (not optimized in the least-squares fitting) were chosen equal to 0.75 while the spin-orbit parameters were left at their *ab initio* values. This low value is suggested by Cowan [53] but we have verified that the use of 0.85 instead of 0.75, would change the final lifetimes by less than 1.8% (except in the case of $9d\ ^3D$ where the modification reaches 3.3%).

The theoretical HFR lifetime values (calculation A) obtained in the present work are summarized in Table I. In a second calculation (calculation B), the following configurations were considered:

$$5d^2 + 5sns\ (n = 6-12) + 5snd\ (n = 5-12) + 5p^2 + 5pnp\ (n = 6-8) + 5pnf\ (n = 4-8) + 5d^2 + 5dns\ (n = 6-8) + 5dnd\ (n = 6-8)$$

and

$$5snp\ (n = 5-12) + 5snf\ (n = 4-12) + 5pns\ (n = 6-8) + 5pnd\ (n = 5-8) + 5dnp\ (n = 6-8) + 5dnf(n = 4-8).$$

Core-polarization effects were incorporated in the calculations by considering the dipole polarizability of the core corresponding to Cd III as computed by Fraga *et al.* [55] but increased by about 10% (in order to obtain a smooth curve when plotting the dipole polarizability vs the ionization degree for the different ions of Cd quoted in the tables of Fraga *et al.*), i.e., $\alpha_d = 8.098 a_0{}^3$. Adopting the value of α_d as computed by Fraga *et al.* [55], would lead to a marginal decrease of the lifetime values (a decrease in fact smaller than 4.5%). The cutoff radius has been calculated as equal to $r_c = 1.240$. The scaling factor adopted for the Slater integrals was also 0.75.

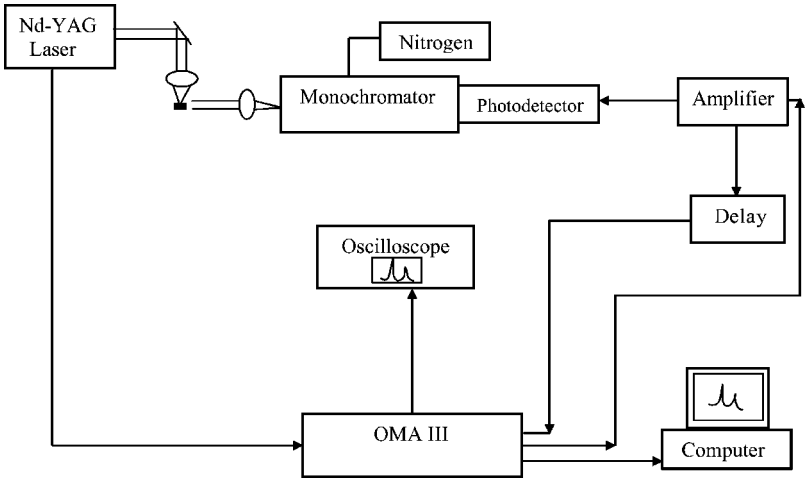

FIG. 6. Experimental setup used for branching ratio measurements. See the text for more details.

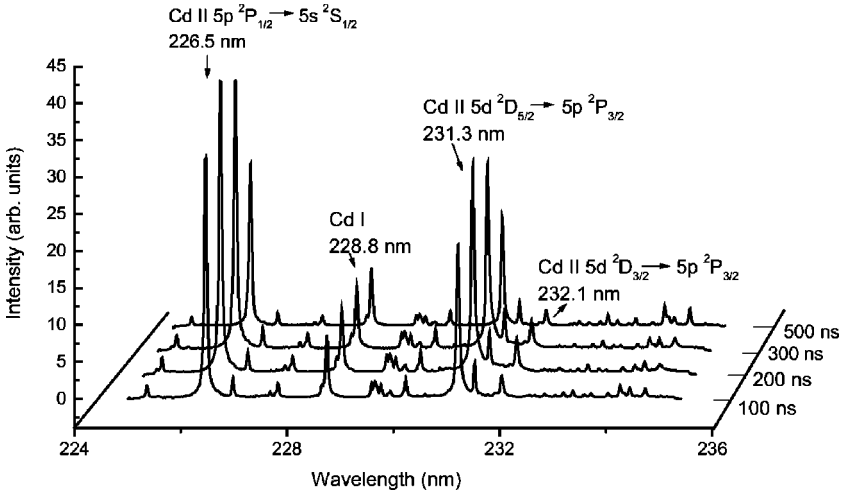

FIG. 7. Time evolution of the Cd spectrum.

The corresponding results are given in Table I under the heading B. The calculated results appear systematically lower (but in a uniform way) than the experimental results. This could be due to an underestimation of the core-polarization effects in the calculation B.

We give in Table II, the weighted transition probabilities and oscillator strengths of the lines depopulating the levels for which the lifetimes have been measured in the present work. We report also the transition probabilities and oscillator strengths (NORM) obtained using the experimental lifetimes and the HFR branching fractions calculated in the present work.

B. HFR calculations in Cd II

The ground state configuration of Cd II is $4d^{10}5s\ ^2S_{1/2}$. The energy levels reported in the NBS compilation [52] are taken essentially from old analyses by von Salis [56], and by Shenstone and Pittenger [57]. They belong to the configurations $4d^{10}ns$ $(n=5-13)$, $4d^{10}np$ $(n=5-13)$, $4d^{10}nd$ $(n=5-14)$, $4d^{10}nf$ $(n=4-11)$, $4d^{10}ng$ $(n=5-11)$, $4d^95s^2$, and $4d^95s5p$.

Several calculations have been performed for Cd II transition probabilities. We used the HFR method as coded by Cowan [53].

In the first calculation (calculation C) the following configurations were considered along the Rydberg series:

$$4d^{10}ns\ (n=5-12)+4d^{10}nd\ (n=5-12)+4d^{10}ng\ (n=5-12)+4d^{10}ni\ (n=7-12)$$

and

$$4d^{10}np\ (n=5-12)+4d^{10}nf\ (n=5-12)+4d^{10}nh\ (n=6-12).$$

Core-polarization (CP) effects were introduced in the calculations in the following way. The static dipole polarizability of Cd III was that computed by Fraga *et al.* [53], i.e., $\alpha_d=5.668\ a_0{}^3$. The cutoff radius r_c was chosen equal to $1.240\ a_0$ and corresponds to the mean value $\langle r\rangle$ of the outermost orbital $4d$ in the configuration $4d^{10}$. As we were interested in Rydberg states, the configuration sets were extended up to $n=12$. The energies of the experimentally known levels are rather well calculated and the agreement theory–experiment was only slightly improved via a fitting procedure. In fact, the levels up to $n=10$ ($n=9$ for nf series) were included in the least-squares fitting, the levels of higher energies being less accurately known (some are indicated with a question mark in the NBS tables).

The scaling factors of the F^k, G^k, and R^k integrals (not optimized in the least-squares fitting) were chosen equal to 0.85 while the spin-orbit parameters were left at their *ab initio* values. The theoretical HFR lifetime values (calculation C) obtained in the present work are summarized in Table III (column 3).

It was also verified that extending the Rydberg series up to $n=16$ introduces in fact a change on the lifetime values smaller than 1%. In addition, increasing the dipole polarizability by 10%, i.e., adopting $\alpha_d=6.235\ a_0{}^3$ and using the same set of configurations as in calculation C does not change the lifetime value of $6s\ ^2S_{1/2}$, hardly changes the values of $5d\ ^2D$ states (increase by about 1.5%) and increases the lifetime values of $5p\ ^2P^o$ states by about 4.0%.

In the next calculation (calculation D), the following configurations were considered:

$$4d^{10}ns\ (n=5-8)+4d^{10}nd\ (n=5-8)+4d^{10}ng\ (n=5-8)+4d^95s^2+4d^95s6s+4d^95s5d+4d^95s6d+4d^95p^2+4d^95p6p+4d^95p4f+4d^95p5f+4d^95p6f+4d^95d^2+4d^95d6s+4d^95d6d$$

and

$$4d^{10}np\ (n=5-8)+4d^{10}nf\ (n=4-8)+4d^95s5p+4d^95s6p+4d^95s4f+4d^95s5f+4d^95p6s+4d^95p5d+4d^95p6d+4d^95d6p+4d^95d4f+4d^95d5f.$$

Core-polarization effects were incorporated in the calculations by considering the dipole polarizability of the core corresponding to Cd IV as computed by Fraga *et al.* [55], i.e.,

TABLE IV. Cd II: oscillator strengths and transition probabilities for the transitions depopulating the levels measured in the present work. We give the HFR results (calculation D) and the values normalized with the experimental lifetimes as measured in the present work. CF: cancellation factor. * Theory E. ** Experimental values, normalized by theory E.

		This work							
		Experiment, gA (10^8 s^{-1})		Theory					
				HFR			NORM		Previous works
Transition	λ (Å)	Exp. 1	Exp. 2	log gf	gA (10^8 s^{-1})	CF	log gf	gA (10^8 s^{-1})	log gf
$5p\ ^2P^o_{1/2}$-$5s\ ^2S_{1/2}$	2265.02	6.2±0.2	6.7±0.8	−0.29	6.68	−0.751	−0.32	6.24	−0.36,[b] −0.36,[c] −0.33[d]
$5p\ ^2P^o_{3/2}$-$5s\ ^2S_{1/2}$	2144.39	16.0±0.5	16.8±2.0	0.04	15.7	−0.746	0.05	16.0	−0.04,[b] −0.03,[c] 0.01[d]
$6s\ ^2S_{1/2}$-$5p\ ^2P^o_{1/2}$	2572.93	3.5±0.5		−0.41	3.97	0.860	−0.45	3.59	−0.51[a]
$6s\ ^2S_{1/2}$-$5p\ ^2P^o_{3/2}$	2748.55	5.2±0.4		−0.14	6.51	0.853	−0.18	5.89	−0.23[a]
$5d\ ^2D_{3/2}$-$5p\ ^2P^o_{1/2}$	2194.55	18.2±1.6		0.27	26.0	0.789	0.14	19.1	0.12[a]
$5d\ ^2D_{3/2}$-$5p\ ^2P^o_{3/2}$	2321.05	4.0±0.3		−0.45	4.41	−0.784	−0.58	3.23	−0.57[a]
$5d\ ^2D_{5/2}$-$5p\ ^2P^o_{3/2}$	2312.75	35.0±0.7	35.3±4.2	0.51	40.0	0.788	0.45	35.5	0.39[a]
$5s^2\ ^2D_{3/2}$-$5p\ ^2P^o_{1/2}$	3250.29	0.14±0.01**		−1.58*	0.15*				
$5s^2\ ^2D_{3/2}$-$5p\ ^2P^o_{3/2}$	3535.67	0.04±0.01**		−2.25*	0.03*				
$5s^2\ ^2D_{5/2}$-$5p\ ^2P^o_{3/2}$	4415.65		0.08±0.01	−1.44*	0.10*				

[a]Quasirelativistic quantum defect orbital formalism with CP [42].
[b]Single-electron approximation with CP [44].
[c]Relativistic single-configuration Hartree-Fock method with CP [45].
[d]Coulomb approximation, Hartree-Slater cor, CP [46].

$\alpha_d = 3.914 a_0^3$ and the cutoff radius has been calculated as equal to $r_c = 1.190$.

The corresponding results are given in Table III under the heading D. Theory and experiment agree within the errors if we except the level $5d\ ^2D_{3/2}$ for which the theoretical result is somewhat smaller than the experiment.

The theoretical f values deduced in the calculation D are reported in Table IV. We report also in the same table the oscillator strengths and transition probabilities normalized by considering the experimental lifetimes as obtained in the present work and the HFR branching fractions. They are quoted in Table IV under the heading NORM. In the case of the calculations of oscillator strengths for Beutler states $4d^9 5s^2\ ^2D_{3/2,5/2}$, we considered configuration interaction among the following configurations:

$$4d^9 5p^2 + 4d^9 5s 6s + 4d^9 6s^2 + 4d^9 5p 6p$$

and

$$4d^9 5s 5p + 4d^9 5s 4f + 4d^9 5s 6p$$

(calculation E).

IV. DISCUSSION OF THE RESULTS

The radiative lifetimes for Cd I, Cd II excited states, measured and calculated in the present work, are presented in Tables I and III. In Tables II and IV, results for oscillator strengths (gf, $g = 2J+1$, where g is the statistical weight of the lower level of the transition) and transition probabilities (gA, $g = 2J+1$, where g is the statistical weight of the upper level of the transition) are presented and are compared with previous results.

A. Cd I

Our lifetime for the $5s5p\ ^1P^o_1$ Cd I level is in a good agreement with the data obtained by beam-foil spectroscopy with multiexponential decay curve analysis [14] and by the Hanle effect method [7]. For the $5sns\ ^3S_1$ series, our results agree well with those derived by the delayed-coincidence method with pulsed electron excitation [17].

Radiative lifetimes of unresolved $nd\ ^3D$ terms have been determined using the beam-foil spectroscopy [14] and the delayed-coincidence method with pulsed electron excitation [16,17]. Our results for $nd\ ^3D_{1,2}$ Cd I states are in a good agreement with these experimental data. Lifetime values for $ns\ ^3S_1$ and $nd\ ^3D_{1,2}$ levels measured by the LIF method [19] are, however, systematically smaller than our measurements. In this experiment a stepwise excitation was realized. Electron excitation of the $5p\ ^3P^o_{0,2}$ Cd I metastable states in a cw discharge was used as a first step, while the laser excitation from these metastable states was performed as a second step. The difference between our data and the experimental results of Ref. [19] might possibly be due to collisional deexcitation in the discharge, used in Ref. [19].

When considering the numerical values of Table I, it is observed that the radiative lifetime values of the excited states belonging to the $nd\ ^3D$ multiplets are increasing with increasing J values. Oscillator strengths for Cd I $5snp\ ^3P^o$-$5snd\ ^3D_{1,2}$ and $5sns\ ^3S_1$-$5snp\ ^3P^o$ transitions calculated in the present work and normalized using the new experimental values of radiative lifetimes are presented in Table II where previous results are also shown. The HFR theoretical lifetimes obtained in the present work appear systematically but coherently smaller than the experimental measurements ex-

cept for the higher members of the *nd* series.

B. Cd II

The Cd II radiative lifetimes are reported in Table III, where they are compared with previous results. Our result for the $6s\ ^2S_{1/2}$ level of Cd II is in a good agreement with the value measured by beam-foil spectroscopy, with multiexponential treatment of decay curves [14]. The lifetime of the same level determined by the delayed-coincidence method [16] with nonselective electron excitation is more than twice larger than our result. There is no information available about this experiment but it can be supposed that the time resolution of the setup was not sufficient for measurement of short lifetimes. This hypothesis is confirmed by the fact that our result for $6s\ ^2S_{1/2}$ agrees well with the single-channel quasiclassical theoretical value [39].

The $5p\ ^2P^o_{1/2,3/2}$ Cd II excited states have been measured by the beam-foil method [14] and the electron-photon coincidence technique [41]. In both experiments, measurements were carried out using an unresolved multiplet. These values are larger than those measured in the present work. The phase-shift method was also used in Ref. [12] for the determination of radiative lifetimes of the $5p\ ^2P^o_{1/2,3/2}$ levels. In this experiment, the cascades from the $4d^95s^2\ ^2D$ levels were taken into account, but not from $6s\ ^2S_{1/2}$, $5d\ ^2D_{3/2,5/2}$ levels (see Fig. 1) from which the main cascade repopulation does occur. This could explain why the radiative lifetimes of Ref. [12] are larger than our results. This is confirmed by the good agreement between our results and those obtained either by the Hanle method applied to cadmium ions produced in a discharge of He-Cd mixture [36] or by the level-crossing method on a fast ion beam (measurement of radiative lifetime of $5p\ ^2P^o_{3/2}$ excited state) [34]. The beam-foil method was also used for life time measurement of $5p\ ^2P^o_{1/2,3/2}$ levels [33] with a multiexponential or an ANDC treatment of the decay curves. The cascades from $6s\ ^2S_{1/2}$ and $5d\ ^2D_{3/2,5/2}$ levels were adequately taken into account. Laser excitation was also employed in the same experiment. Both the results deduced using nonselective and selective excitation agree within the error limits with our measurements. The data from Ref. [33] presented in Table III, correspond to selective excitation.

An unresolved multiplet was used in a beam-foil experiment to measure radiative lifetimes of $5d\ ^2D_{3/2,5/2}$ levels [14]. Cascade repopulation is the possible explanation for the discrepancy observed between the value of Ref. [14] and our measurement. A level crossing experiment on a fast ion beam was applied for measurement of radiative lifetimes of $5d\ ^2D_{3/2}$ and of the unresolved term $5d\ ^2D$ [34]. These results agree, within the error bars, with our measurements. The beam-foil method was applied for measurements of radiative lifetimes of $5d\ ^2D_{3/2,5/2}$ states, using multiexponential treatment of decay curves [33]. These results were included in the ANDC analysis of the decay of $5p\ ^2P^o_{1/2,3/2}$ levels, performed in this work.

The agreement theory (i.e., HFR method) experiment for Cd II radiative lifetimes obtained in the present work is good; the theoretical result appears, however, somewhat smaller than the experimental one for the $5d\ ^2D_{3/2}$ level. In Table IV, oscillator strengths and transition probabilities of 5*s*-5*p*, 5*p*-6*s*, 5*p*-5*d*, and $5p$-$4d^95s^2$ transitions, calculated and measured in the present work as well as normalized by experimental lifetimes are presented and compared with previous results. The experimental transition probability data, obtained in the present work, presented under the headings "Exp. 1" and "Exp. 2" agree very well, with the exception of transitions from $5d\ ^2D_{3/2}$ state.

In Ref. [45], several theoretical approaches were used for oscillator strength calculation of resonance $5s\ ^2S_{1/2}$-$5p\ ^2P^o_{1/2,3/2}$ spectral lines but, in Table IV, we report only the RHF+CP results. Similar considerations apply to the results of Ref. [42] (5*p*-5*d* and 5*p*-6*s* transitions) and the results reported in Table IV were obtained with the quasirelativistic quantum defect orbital formalism with polarization effects included. In both cases, large discrepancies are observed when comparing these results with our experimental and theoretical values. This emphasizes the difficulty to perform accurate calculations of radiative parameters in the heavy neutral or singly ionized atoms.

V. CONCLUSIONS

The results of the present experiment are compared with theoretical calculations of lifetimes using a multiconfigurational relativistic Hartree-Fock method, taking core-polarization effects into account. A good agreement between the measured and the calculated lifetime values is obtained. As both in Cd I and Cd II, transition probabilities and oscillator strengths available in the literature concern only a limited number of transitions, generally connecting levels of low excitation (see, e.g., Ref. [7]), we have deduced in the present work a set of transition probabilities and oscillator strengths for the transitions depopulating the levels of interest. For that purpose, we have combined, for Cd I the experimental lifetimes and the theoretical branching fractions and, for Cd II, the experimental lifetimes and measured branching fractions. The agreement observed between the normalized Cd II transition probabilities and those deduced from LIBS measurements strongly supports the new set of results proposed in the present paper.

ACKNOWLEDGMENTS

The experimental part of this work is supported by the European Community, under the program "Access to Research Infrastructures," Contract No. HPRI-CT 1999-00041. K. Blagoev, G. Malcheva, V. Pentchev, and E. Biémont are grateful to their colleagues from the Lund Laser Center for their kind hospitality and support. We would like to thank Professor M. C. Sanchez Trujillo and her group Dpto. Fisica de los Materiales, Univ. Complutense de Madrid for making in their laboratory the necessary alloys for this experiment.

[1] E. Biémont, H. P. Garnir, P. Palmeri, P. Quinet, Z. S. Li, Z. G. Zhang, and S. Svanberg, Phys. Rev. A **64**, 022503 (2001).
[2] D. C. Morton, Astrophys. J., Suppl. Ser. **130**, 403 (2000).
[3] Z. S. Li, H. Lundberg, G. M. Wahlgren, and C. M. Sikström, Phys. Rev. A **62**, 032505 (2000).
[4] H. Xu and Z. Jiang, Phys. Rev. B **66**, 035103 (2002).
[5] M. Zemansky, Z. Phys. **72**, 587 (1931).
[6] H. D. Koening and A. Ellett, Phys. Rev. **39**, 576 (1932).
[7] A. Lurio and R. Novick, Phys. Rev. **134**, A608 (1964).
[8] B. Laniepce, J. Labias, and M. Chantepie, Opt. Commun. **19**, 92 (1976).
[9] B. Laniepce, J. Phys. (France) **31**, 439 (1970).
[10] B. Laniepce, M. Chantepie, J. Labias, and D. David, Opt. Commun. **23**, 83 (1977).
[11] F. W. Byron, Jr., M. N. McDermott, and R. Novick, Phys. Rev. **134**, A615 (1964).
[12] S. R. Baumann and W. H. Smith, J. Opt. Soc. Am. **60**, 345 (1970).
[13] H. W. Webb and H. A. Messenger, Phys. Rev. **66**, 77 (1944).
[14] T. Andersen and G. Sørensen, J. Quant. Spectrosc. Radiat. Transf. **13**, 369 (1973).
[15] B. Cheron, J. Jarosz, and P. Verisch, J. Phys. B **13**, 2413 (1980).
[16] A. R. Schaefer, J. Quant. Spectrosc. Radiat. Transf. **11**, 197 (1971).
[17] Ya. F. Verolainen and V. I. Privalov, Opt. Spectrosc. **46**, 238 (1979).
[18] L. Frasinski and T. Duhnalik, J. Phys. B **14**, L711 (1981).
[19] H. Kerkhoff, M. Schmidt, U. Teppner, and P. Zimmermann, J. Phys. B **13**, 3969 (1980).
[20] D. Cvejanovic, A. Adams, and G. C. King, J. Phys. B **9**, 1657 (1976).
[21] J. P. A. van Hengstum and J. A. Smit, Physica (Amsterdam) **22**, 86 (1956).
[22] N. P. Penkin and T. P. Redko, Opt. Spectrosc. **9**, 360 (1960).
[23] J. Ahmad, U. Greismann, I. Martin, W. Dussa, M. A. Baig, and J. Hormes, J. Phys. B **29**, 2963 (1996).
[24] A. Schnitzer, K. Hollenberg, and W. Behmenburg, Opt. Commun. **48**,116 (1983).
[25] B. Warner, Mon. Not. R. Astron. Soc. **140**, 53 (1968).
[26] P. F. Gruzdev, Opt. Spectrosc. **22**, 169 (1967).
[27] T. M. Helliwell, Phys. Rev. **135**, A325 (1964).
[28] C. Lavin and I. Martin, J. Quant. Spectrosc. Radiat. Transf. **52**, 21 (1994).
[29] V. A. Zilitis, Opt. Spectrosc. **31**, 161 (1971).
[30] D. Kulaga and J. Migdalek (private communication).
[31] A. Hibbert, Nucl. Instrum. Methods Phys. Res. **202**, 323 (1982).
[32] J. Migdalek, Phys. Scr., T **T100**, 47 (2002).
[33] E. H. Pinnington, J. J. van Hunen, R. N. Gosselin, B. Guo, and R. W. Berends, Phys. Scr. **49**, 331 (1994).
[34] T. Andersen, O. Poulsen, and P. S. Ramanujam, J. Quant. Spectrosc. Radiat. Transf. **16**, 521 (1976).
[35] F. H. K. Rambow and L. D. Schearer, Phys. Rev. A **14**, 1735 (1976).
[36] J. Hamel and J. P. Barrat, Opt. Commun. **10**, 331 (1974).
[37] J. Hamel, J. Margerie, and J. P. Barrat, Opt. Commun. **12**, 409 (1974).
[38] Y. F. Verolainen and V. I. Privalov, Opt. Spectrosc. **48**, 245 (1980).
[39] B. I. Prosihin, N. N. Bezuglov, and Ja. F. Verolainen, Opt. Spectrosc. **68**, 251 (1990).
[40] E. Geneux and B. Wandres-Vincenz, Phys. Rev. Lett. **3**, 422 (1959).
[41] D. A. Shaw, A. Adams, and G. C. King, J. Phys. B **8**, 2456 (1975).
[42] A. Lavin, M. A. Almarz, and I. Martin, Z. Phys. D: At., Mol. Clusters **34**, 143 (1995).
[43] H. S. Chou and W. R. Johnson, Phys. Rev. A **56**, 2424 (1997).
[44] B. N. Chichkov and V. P. Shevelko, Phys. Scr. **23**, 1055 (1981).
[45] J. Migdalek and W. E. Baylis, J. Quant. Spectrosc. Radiat. Transf. **22**, 113 (1979).
[46] J. A. Cardelli, S. R. Federman, D. L. Lambert, and C. E. Theodosiou, Astrophys. J. **416**, L41 (1993).
[47] S. Schiemann, W. Hogervorst, and W. Ubachs, IEEE J. Quantum Electron. **34**, 407 (1998).
[48] L. C. Popovic, I. Vince, and M. S. Dimitrijevic, Astron. Astrophys., Suppl. Ser. **102**, 17 (1993).
[49] H. L. Xu, S. Svanberg, P. Quinet, H. P. Garnir, and E. Biemont, J. Phys. B **36**, 4773 (2003).
[50] A. P. Thorne, *Spectrophysics* (Chapman & Hall, London, 1988).
[51] A. Corney, *Atomic and Laser Spectroscopy* (Clarendon, Oxford, 1977).
[52] Ch. E. Moore, *Atomic Energy Levels* (National Bureau of Standards, Washington, 1958), Vol. 3.
[53] R. D. Cowan, *The Theory of Atomic Structure and Spectra* (University of California Press, Berkeley, 1981).
[54] P. Quinet, P. Palmeri, E. Biémont, M. M. McCurdy, G. Rieger, E. H. Pinnington, M. E. Wickliffe, and J. E. Lawler, Mon. Not. R. Astron. Soc. **307**, 934 (1999).
[55] S. Fraga, J. Karwowski, and K. M. S. Saxena, *Handbook of Atomic Data* (Elsevier, Amsterdam, 1976).
[56] G. von Salis, Ann. Phys. (Leipzig) **76**, 153 (1924).
[57] A. G. Shenstone and J. T. Pittenger, J. Opt. Soc. Am. **39**, 220 (1949).